How to cite: Angew. Chem. Int. Ed. 2024, e202405983
doi.org/10.1002/anie.202405983

On-Surface Synthesis Hot Paper

Controlling On-Surface Photoactivity: The Impact of π-Conjugation in Anhydride-Functionalized Molecules on a Semiconductor Surface

Federico Frezza, Ana Sánchez-Grande, Sofia Canola, Anna Lamancová, Pingo Mutombo, Qifan Chen, Christian Wäckerlin, Karl-Heinz Ernst, Matthias Muntwiler, Nicola Zema, Marco Di Giovannantonio,* Dana Nachtigallová,* and Pavel Jelínek**

Abstract: On-surface synthesis has become a prominent method for growing low-dimensional carbon-based nanomaterials on metal surfaces. However, the necessity of decoupling organic nanostructures from metal substrates to exploit their properties requires either transfer methods or new strategies to perform reactions directly on inert surfaces. The use of on-surface light-induced reactions directly on semiconductor/insulating surfaces represents an alternative approach to address these challenges. Here, exploring the photochemical activity of different organic molecules on a SnSe semiconductor surface under ultra-high vacuum, we present a novel on-surface light-induced reaction. The selective photodissociation of the anhydride group is observed, releasing CO and CO_2. Moreover, we rationalize the relationship between the photochemical activity and the π-conjugation of the molecular core. The different experimental behaviour of two model anhydrides was elucidated by theoretical calculations, showing how the molecular structure influences the distribution of the excited states. Our findings open new pathways for on-surface synthesis directly on technologically relevant substrates.

Introduction

The on-surface synthesis (OSS) method is nowadays widely used to grow low-dimensional carbon-based nanomaterials. Several 0D, 1D and 2D covalently bonded molecular architectures have been synthetized and characterized at the atomic scale.[1–3] In the OSS context, most of the reactions are thermally induced on coinage metal surfaces under ultra-high vacuum (UHV) conditions, where the important catalytic role of metallic substrates opens new reaction pathways during thermal activation.[4–6] However, in order to fully exploit the properties of the organic products in view of applications, non-metallic substrates must be considered. In the last years a few nanostructures, in particular graphene nanoribbons, were successfully integrated into electronic devices such as field-effect transistors.[7,8] Different strategies are available to transfer organic nanostructures from the metal surface and deposit them on technologically relevant substrates.[9] However, they often consist of complex procedures that do not always fully preserve the structural integrity and properties of the material, in addition to the difficult scalability of the process. Hence, the development

[*] F. Frezza, Dr. A. Sánchez-Grande, Dr. S. Canola, Dr. P. Mutombo, Q. Chen, Prof. K.-H. Ernst, Prof. P. Jelínek
Institute of Physics
Czech Academy of Sciences
Cukrovarnická 10, 16200, Prague 6, Czech Republic
E-mail: sanchez@fzu.cz
jelinekp@fzu.cz

F. Frezza
Faculty of Nuclear Sciences and Physical Engineering
Czech Technical University in Prague
Břehová 78/7, 11519 Prague 1, Czech Republic

A. Lamancová, Dr. D. Nachtigallová
Institute of Organic Chemistry and Biochemistry
Czech Academy of Sciences
Flemingovo náměstí 542/2, 160 00 Prague, Czech Republic
E-mail: dana.nachtigallova@uochb.cas.cz

Prof. Dr. C. Wäckerlin
Institute of Physics
Swiss Federal Institute of Technology Lausanne (EPFL)
CH-1015 Lausanne, Switzerland

Prof. Dr. C. Wäckerlin, Dr. M. Muntwiler
Paul Scherrer Institute (PSI)
5232 Villigen PSI, Switzerland

Prof. K.-H. Ernst
Empa, Swiss Federal Laboratories for Materials Science and Technology
8600 Dübendorf, Switzerland

Dr. N. Zema, Dr. M. Di Giovannantonio
CNR - Istituto di Struttura della Materia (CNR-ISM)
via Fosso del Cavaliere 100, 00133, Rome, Italy
E-mail: marco.digiovannantonio@ism.cnr.it

Dr. D. Nachtigallová
IT4Innovations
VŠB-Technical University of Ostrava,
17. listopadu 2172/15, 708 00 Ostrava-Poruba, Czech Republic

of new strategies for the OSS of nanostructures directly on semiconducting or insulating substrates is desirable in view of prototypical device fabrication for future applications in organic electronics. Few efforts have been devoted to the synthesis of carbon nanostructures directly on bulk insulator surfaces, such as TiO_2 or calcite.[10,11] One of the main limitations of this approach in the case of thermally activated reactions is the likely desorption of the precursors before any reaction is initiated, due to their low adsorption energy and the lack of catalytic activity from the substrate.[12,13]

In view of these restrictions, on-surface photochemistry offers a valid solution to promote chemical processes on non-metallic substrates, even in mild reaction conditions. Photons can both form and break bonds, and their energy, intensity, and polarization can easily be tuned. While traditional organic photochemistry is a mature field whose origins trace more than a hundred years back,[14] its on-surface counterpart remains still largely unexplored. On-surface photochemistry permits to carry on reactions on inert surfaces and on large areas, opening reaction pathways that are not thermally accessible.[15] While some examples of light-induced reactions on surfaces have been reported, such as diacetylene polymerization,[16,17] carbon-halogen activation,[18–21] alkyne coupling[22,23] and [4+4] cycloaddition,[24] the synthesis of nanostructures directly on semiconducting or insulating surfaces is still challenging.[25–28]

The selective photolysis and pyrolysis of anhydrides has proven to be a suitable approach for the formation of arynes, as schematically shown in Figure 1a for the case of the phthalic anhydride (PhA).[29–34] Many organic synthesis experiments have been carried out in solution, gas-phase and in inert gas matrices at cryogenic temperature. Several phthalic anhydride derivatives were demonstrated to be photochemically active upon UV light irradiation inducing the dissociation of the anhydride group and leading to the loss of CO and CO_2, forming highly reactive arynes that can occasionally di- or trimerize. Cycloaddition reactions involving arynes are widely used for the synthesis of a large variety of nanographenes.[35] Thus, the possibility of generating reactive arynes intermediates via on-surface photodissociation of the anhydride group offers a convenient strategy for the synthesis of polycyclic aromatic compounds on surfaces, through a convenient design of the precursor.

The goal of this work is to expand the toolbox of OSS presenting a new light-induced reaction on a non-metallic

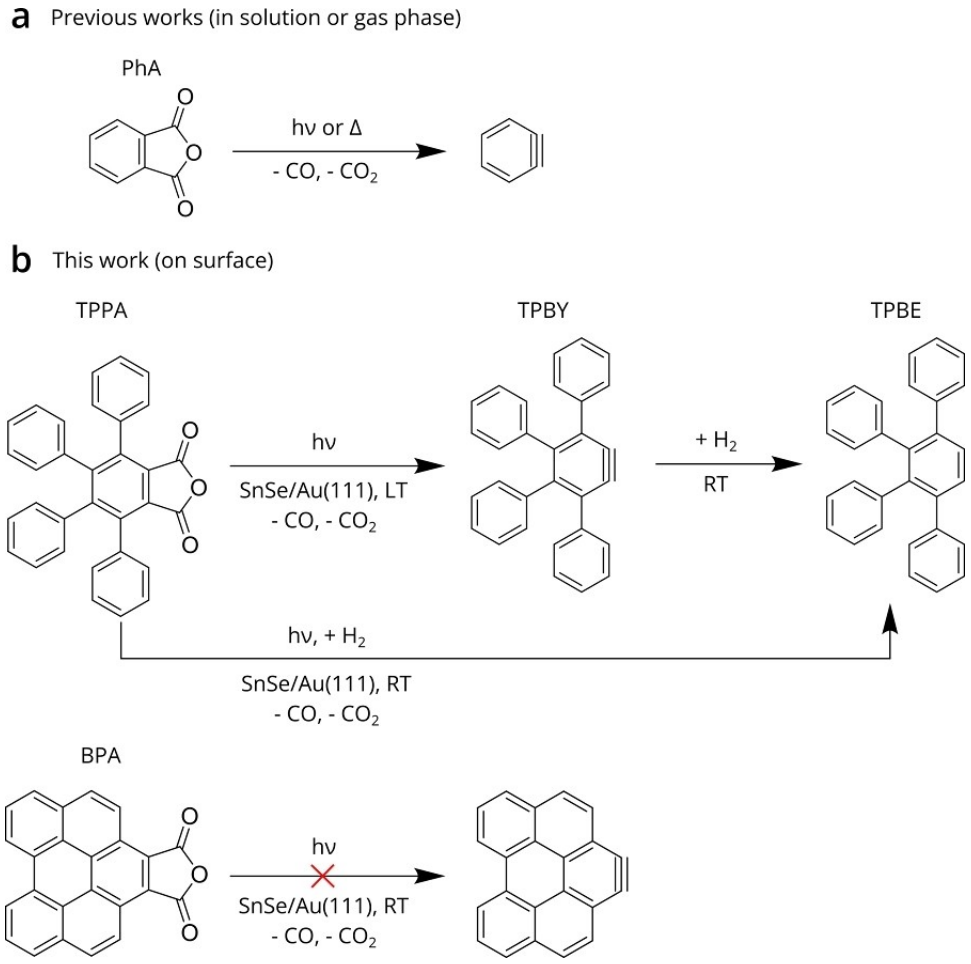

Figure 1. Chemical sketches of a) the previously reported photolysis or pyrolysis of PhA,[29,30] and b) the photolysis of TPPA on the SnSe surface reported in this work and the unsuccessful reaction of BPA.

surface. To this aim, we investigated the photoactivity of two different precursors equipped with the anhydride group on a semiconductor surface by means of low-temperature scanning tunneling microscopy (LT-STM), non-contact atomic force microscopy (nc-AFM) and X-ray photoelectron spectroscopy (XPS), supported by quantum-chemical calculations. Figure 1b summarizes the photolysis reactions reported in this work. The tetraphenylphthalic anhydride (TPPA) precursor consists in a phthalic anhydride backbone with four phenyl substituents, that increase the molecular weight helping the adsorption on the surface. Conversely, benzo[*ghi*]perylene-1,2-dicarboxylic anhydride (BPA) is a planar molecule presenting a polycyclic aromatic hydrocarbon (PAH) core. Here, we experimentally revealed the selective photodissociation of the anhydride group from the precursor TPPA on the semiconductor SnSe surface under UHV conditions. On the contrary, we observed the lack of photoactivity in the case of the BPA precursor presenting a π-conjugated core. We rationalized the experimental findings by theoretical simulations predicting a first excited state with strong dissociative character for the TPPA. In the case of BPA, the higher delocalization of the π-conjugated core has a direct impact on the order of the excited states and hence on its photochemical behaviour.

Results and Discussion

We employed semiconducting SnSe thin films epitaxially grown on Au(111) as an inert surface, which contain very low number of native defects as previously reported.[36] TPPA molecules were initially sublimed onto the SnSe surface kept at room temperature (RT). Figure 2a shows an overview STM image where the SnSe surface is partially

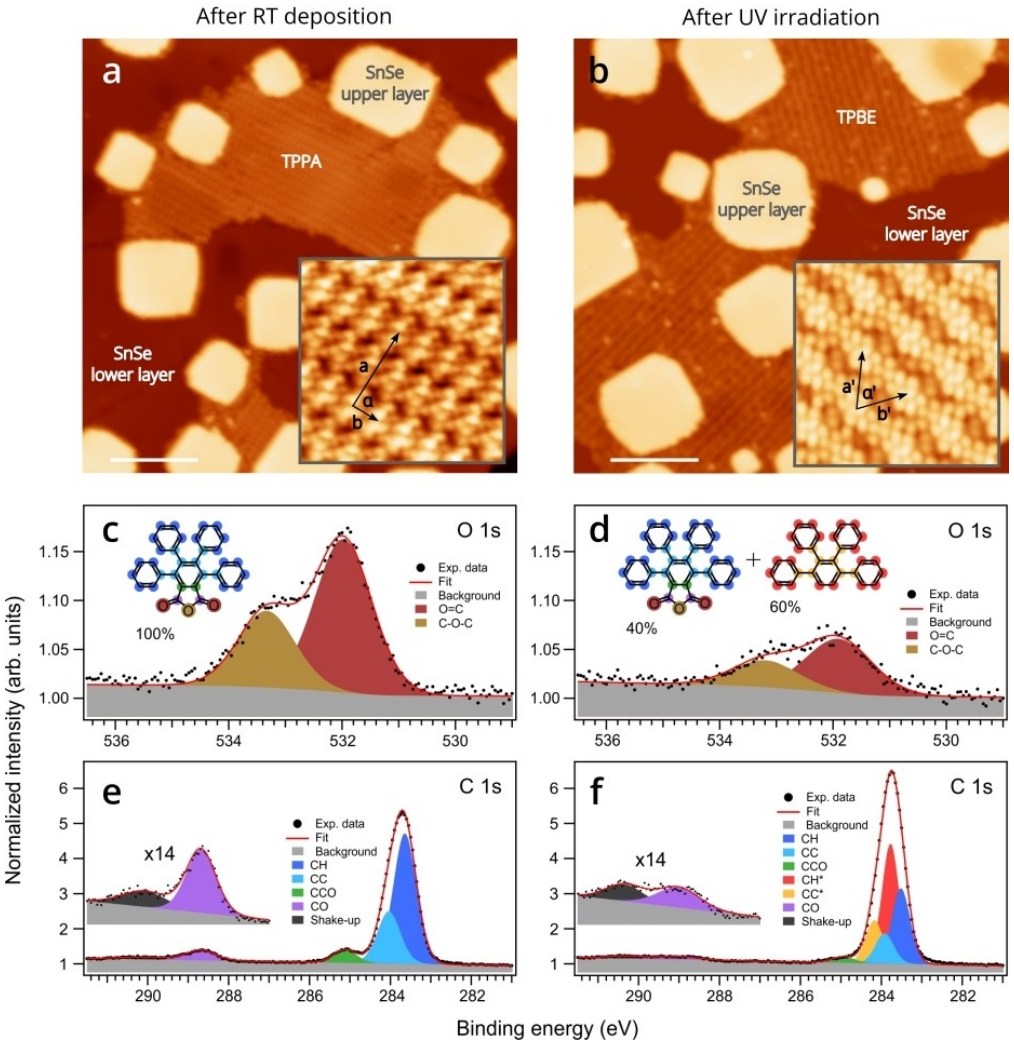

Figure 2. STM overview images of a) the pristine TPPA deposited on SnSe/Au(111) (V = 2 V, I = 20 pA, scale bar = 20 nm) and b) the sample after UV irradiation at RT (V = 2 V, I = 10 pA, scale bar = 20 nm). Insets show high resolution STM images (V = −2 V, I = 20 pA, 8×8 nm^2 for both images) and the self-assembly unit cell. c,d,e,f) Normalized high-resolution XPS spectra acquired using synchrotron radiation with photon energy of 650 eV and 425 eV for O 1s and C 1s, respectively. O 1s and C 1s core levels are shown c,e) before and d,f) after UV irradiation at RT. Colored dots in the Scheme highlight carbon atoms in different chemical environments, and their colors correspond to those of the fitting components (see Table S1 for the fitting parameters).

covered by TPPA molecules forming well-ordered self-assembled islands. The molecules tend to adsorb onto the lower SnSe layer, and some clean upper layer SnSe islands are also visible.. The adsorption energy of TPPA on SnSe is limited and complete molecular desorption is observed after annealing at 150 °C. The inset of Figure 2a presents a zoomed-in STM image on the molecular self-assembly acquired at negative bias from which we can infer the rectangular unit cell parameters $a = 3.3$ nm, $b = 1.1$ nm, $\alpha = 90°$. In the TPPA molecule, the phenyl groups are usually twisted respect to the plane of the central ring due to the steric repulsion, thus adopting a "propeller" configuration in crystals.[37] Density functional theory (DFT) simulations of a single TPPA molecule on the SnSe surface show how the propeller configuration, with the phenyl groups almost perpendicular to the surface plane, is retained also on the surface. The relaxed TPPA structure is shown in Figure S1, together with experimental and simulated STM/nc-AFM images.

The sample was then irradiated for 15 hours with $\lambda = 280$ nm at RT using a UV LED (details about the illumination setup in the SI). It is worth mentioning that no thermal heating was detected due to the illumination, so we could rule out any temperature-induced process. After illumination, the molecules were still found arranged in a striped self-assembly (see STM overview in Figure 2b) but presented a completely different appearance compared to the pristine TPPA molecule. The STM image in the inset of Figure 2b, acquired at negative bias, reveals a new contrast consisting in many lobe-like features and an oblique unit cell with $a' = 2.2$ nm, $b' = 2.0$ nm and $\alpha' = 68°$. After illumination most of the molecules on the sample display this new appearance in STM, which we tentatively assigned to the presence of a chemically different species induced by UV irradiation. Thus, we assigned this change in STM appearance to the presence of a chemically different species induced by UV irradiation, as corroborated by nc-AFM measurements (Figure S2). As anticipated in Figure 1, the illumination of anhydrides induces the loss of CO and CO_2 molecules and the photogeneration of arynes. For direct comparison between pristine TPPA and the photoactivated product we illuminated a new TPPA on SnSe sample for 3 hours at 280 nm (see Figure S3). In this case, the coexistence of the two chemical species can be recognized, where some small molecular islands are photoactivated, while the large islands remain unreacted, suggesting a cooperative effect, containing some single molecules photoactivated in the TPPA assembly (see Figure S3c and d).

In order to confirm the chemical composition of the TPPA precursor and its photochemical transformation, we performed high resolution X-ray photoelectron spectroscopy (HR-XPS) experiments using synchrotron radiation as the photon source. Figure 2c,d,e,f shows the normalized photoemission spectra for the O 1s and C 1s core levels of the TPPA molecules on SnSe/Au(111) before and after the UV irradiation at RT. The insets show the molecular structures of precursor and product, highlighting the chemically inequivalent atoms with different colours, the same of the respective peaks in the fits. In the case of the pristine TPPA, the O 1s peak (Figure 2c) can be fitted with two components with binding energies (BE) of 532.0 eV and 533.3 eV in a 2:1 ratio, as expected for the two chemically different oxygen atoms in the anhydride group.[38] The C 1s spectrum (Figure 2e) presents an intense peak around 283.8 eV, a shoulder at 285.1 eV, and a minor signal at higher BE, magnified in the inset. The main peak can be deconvoluted into two components, corresponding to the sp^2 carbon atoms in C–H and C–C form, located at 283.6 eV and 284.0 eV, respectively (dark and light blue peaks). The shoulder at 285.1 eV (green peak) likely arises from the two carbon atoms adjacent to the anhydride, which have a different chemical environment. We assign the high BE component (288.7 eV, violet) to the two carboxylic carbon atoms in the anhydride group.[39] The fit was carried out fixing the ratio between the contributions from the chemically different carbon atoms (all the fit parameters are reported in Table S1). This analysis thus demonstrates that the TPPA is intact on the SnSe surface. After illumination, the intensity of the O 1s signal drops visibly. However, it can still be fitted with the same two components in a 2:1 ratio. This points to the loss of CO and CO_2 from the TPPA precursor and subsequent desorption from the SnSe surface, while the remaining molecules stay in their intact, pristine form. From the variation of the O/C ratio before and after light exposure, we estimated that 60 % of the molecules have reacted. In an analogous experiment in our in-house XPS setup, we demonstrated that the reaction can reach a conversion as high as 91 % after 16 hours (Figure S4). Although we cannot exclude that the reaction would proceed further with longer light exposure time, the photoconversion from XPS experiment agrees with the STM data in Figure S4 and it is also in agreement with the yield of other on-surface photoinduced reactions.[24] To carry out the fit of the C 1s spectrum after irradiation (Figure 2f), we considered the presence of 40 % of intact molecules on the surface, as derived from the O 1s signal. In addition to the signals related to the intact molecules, the fit shows the appearance of two new components (red and yellow peaks) at 283.8 eV and 284.2 eV respectively, which account for the C–H and C–C carbon atoms in the final product. Here, the peak ratio is 11:4, as expected for tetraphenylbenzene (TPBE). The C 1s area increases after the illumination by 5 %. This increase can be attributed to two main factors, (i) a small contamination of the sample from other sources in the analysis chamber (e.g. hot filaments) and (ii) inequivalent photoelectron diffraction effects for the two molecular species. Altogether, XPS measurements point to the formation of TPBE as the final product, after the successful photolysis of the anhydride group.

Once the photolysis of the anhydrides has been confirmed by XPS and STM measurements, we performed additional experiments to get more insight into the mechanism. First, we investigated the response to different wavelengths (see Figure S5). After illumination at 450 nm and 360 nm the TPPA molecules remain unreacted, suggesting that the photoactivation process consists of a purely intramolecular excitation mechanism. Nevertheless, we cannot disregard the plausible contribution of substrate-mediated

photoactivation. Then, a control experiment on the bare Au(111) (see Figure S6) shows how TPPA does not preserve its structural stability at RT after 15 hours in dark conditions, highlighting the importance of employing inert surfaces.

Interestingly, the photolysis of TPPA and generation of TPBE can also be achieved following a stepwise process by irradiation at low temperature and subsequent annealing to RT, as illustrated in Figure S7. We monitored the process by STM and XPS measurements at each reaction step. After LT irradiation using a laser source, we already observed a change in STM contrast, assigned to the formation of the intermediate tetraphenyl benzyne (TPBY) after the loss of the anhydride group as CO and CO_2 molecules. Arynes generation by local tip manipulation has already been demonstrated on the NaCl surface at cryogenic temperatures and under UHV conditions.[40] We also note the presence of some mobile species on the surface, visible in the STM images as fuzzy lines (Figure S7e), which can be explained with the presence of CO and CO_2 molecules adsorbed on the surface while the sample is kept at LT. Deconvolution of the O 1s spectrum in Figure S3b, supports the presence of co-adsorbed CO and CO_2 after LED irradiation (and dissociation) at LT. These species desorb from the surface when the sample is annealed to RT and only the components of the intact TPPA leftover is seen in the XPS signal (Figure S7c). In agreement with our interpretation, STM images acquired after annealing the sample to RT for 30 minutes only show TPBE islands (Figure S7f), formed after the hydrogenation of TPBY due to the presence of residual hydrogen in the UHV chamber.[41,42]

Next, we investigated the BPA precursor, also equipped with the same anhydride group, and containing the PAH core with a higher degree of π-conjugation compared to TPPA. We deposited the BPA molecules onto the SnSe surface, obtaining ordered self-assembled molecular islands. STM and nc-AFM images (Figure S8) show a regular arrangement in rows and the planar molecular geometry allows bond-resolved imaging revealing a head-to-tail configuration. Nevertheless, RT illumination at 280 nm or 350 nm for several hours (calculated BPA absorption spectrum in Table S3) did not lead to any apparent structural or chemical change, showing no photoactivity of the BPA molecule.

Although the photochemical activity of anhydrides has been proven during the last century, and here it is also demonstrated on an inert surface by the TPPA precursor, the lack of photochemical activity of the BPA precursor anticipates some limitations. To rationalize the experimental findings and clarify the difference in photochemical activity between TPPA and BPA, we performed theoretical calculations. Namely, we employed the second-order algebraic-diagrammatic construction (ADC(2)) method with cc-pVDZ basis set.[43,44] Due to the considerable computational demands of the ADC(2) method, making the calculations of the original systems intractable, we used model systems with simplified chemical structures. All calculations were performed in the gas phase. For TPPA, we employed the phthalic anhydride (PhA) molecule representing the core of the TPPA molecule (see Figure S9). To mimic BPA, we selected pyrene anhydride (PyA), as a minimalistic representation of the π-conjugated unit (see Figure S10). The validity of this approximation is confirmed by the similarity in character and ordering of the lowest excited states of the experimentally studied molecules and their models, Figure 3 and Tables S2,3.

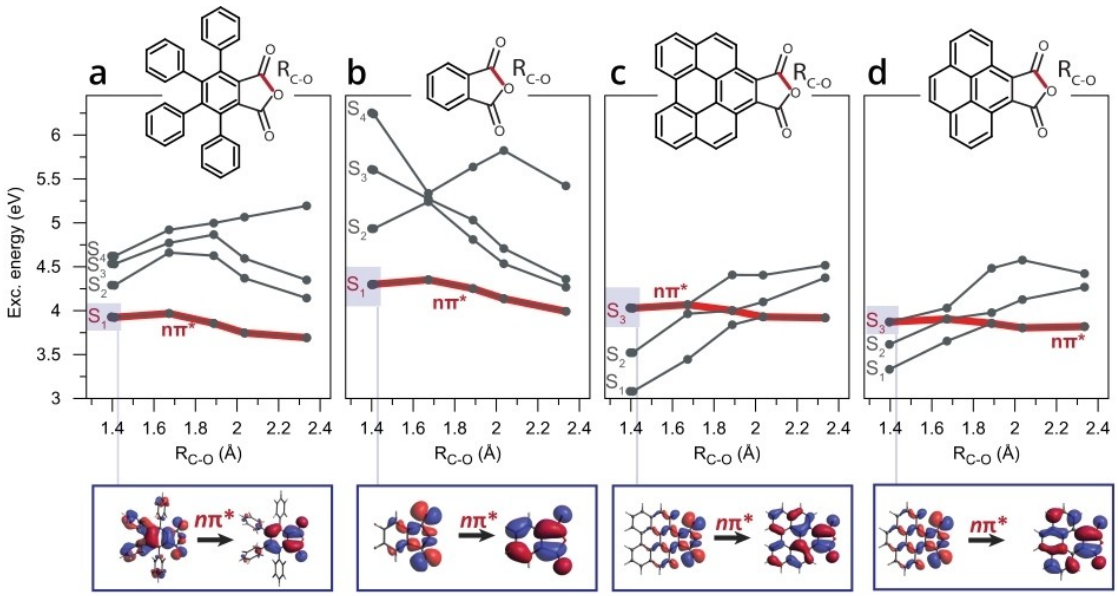

Figure 3. Potential energy surfaces calculated at the optimized ground-state geometries, while scanning along C–O bond R_{C-O}, of a) TPPA, b) PhA, c) BPA and d) PyA. The energies and electronic transitions of the excited states are obtained at the relevant S_0 geometries. The dissociative character of the nπ* state is indicated by the red bold line and the other excited states (indicated in gray) are mostly due to the transitions within the π frame. The molecular orbitals involved in the electronic transitions of nπ* states are also pictured at the bottom panel.

Tables S2,3 summarize the character of the excited states for the optimized geometries in the ground states. Our investigation revealed that for TPPA and PhA molecules, the S_1 state corresponds to a spectroscopically dark n→π* state that results from the transition of the electron from lone pair orbitals localized on the oxygen atoms to an unoccupied π* molecular orbital. The following two excited states S_2 and S_3 correspond to the transition between π→π* states involving transitions from HOMO and HOMO-1, localized on phenyl rings, to LUMO, mainly localized on the maleic anhydride fragment (molecular orbitals are shown in Figure S9). The S_2 and S_3 states exhibit considerable oscillator strengths and are most likely involved in the excitation following illumination at 280 nm, in line with the experimentally observed photodissociation process in the TPPA molecule. On the contrary, BPA and PyA show quite different characteristics of the excitation spectra. The lowest excitation S_1 and S_2 states have π→π* character followed by a dark n→π* state (S_3), see Table S3. Note that our calculations did not consider the triplet states. The singlet-triplet transitions operate on longer timescales, and we assumed that such processes are unlikely to compete with relaxations that occur on the timescale of a few picoseconds.

According to Kasha's rule,[45] we assumed fast internal energy conversion processes from higher absorbing excited states to the lowest excited state. Thus, the character of the lowest excited state determines the response of the system upon the photoexcitation. Figure 3a,b compare the excitation energies of S_1–S_4 states calculated at the ground state optimized structures of TPPA and PhA while scanning the dissociation along C–O bond (R_{C-O}), i.e., increasing R_{C-O} bond length and keeping it fixed while optimizing all other parameters. In both cases, the S_1 state (red bold curve) maintains n→π* character along the entire scan, with descending energy values for increasing R_{C-O}, showing a dissociative character. In the case of BPA/PyA, we observe an entirely different scenario, as shown in Figure 3c,d. The energy of the π→π* S_1 and S_2 states increases as R_{C-O} elongates, which inhibits a spontaneous rupture of the C–O bond. Note that S_1 adopts n→π* character only at large R_{C-O} values (about 1.8 Å for PyA and 2.0 Å for BPA).

The optimization of S_1 state of PhA spontaneously led to the structure in which the five-membered ring opens due to a dissociation of R_{C-O}. Note that the resulting minimum is characterized by a negative excitation energy which indicates the existence of conical intersections. In such scenario, the applicability of the single-reference-based ADC(2) method becomes limited. Therefore, to validate the dissociative character of the n→π* state (S_1), the geometry of PhA was optimized on the S_1 potential energy surface (PES) while scanning along R_{C-O} bond. Figure 4a shows that the energy of S_1 state gradually decreases approaching the energy of the ground state (black curve) and indicating the opening of the five-membered ring by a dissociation of the C–O bond. The changes in the character of S_1–S_4 electronic transitions are illustrated in more detail in Figure S11a, where the electronic transitions while scanning along R_{C-O} are represented.

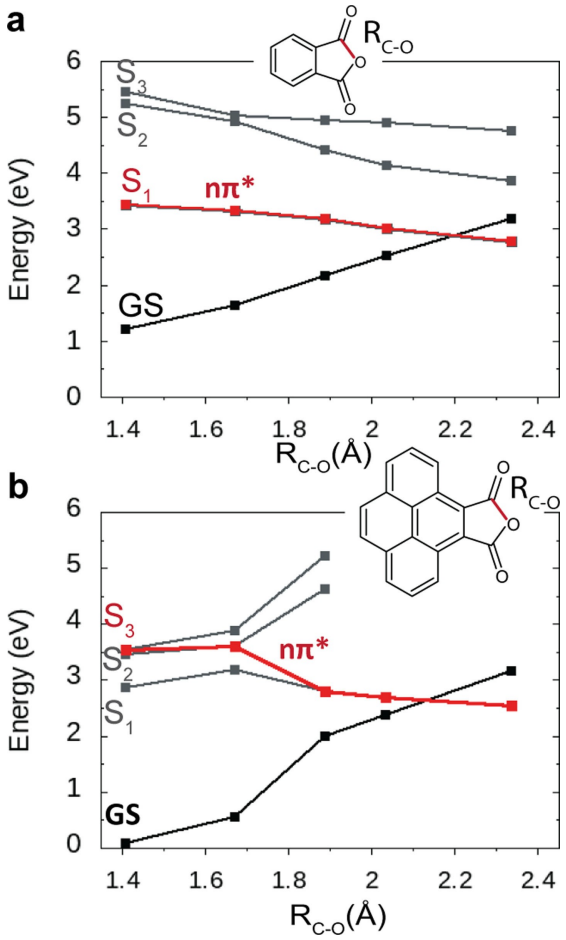

Figure 4. Potential energy surfaces calculated at the optimized geometries of S_1 states, while scanning along R_{C-O}, of a) PhA and b) PyA. The energies of the ground (GS) and excited states are obtained at the relevant S_1 geometries. The dissociative character of the nπ* state is represented by the red bold line.

Contrary to PhA, the optimization of the S_1–S_4 excited states of PyA always led to stable minima without any indication of a possible dissociation. This stability persists even in the case where the R_{C-O} bond has been extended by 0.1 Å. Additionally, we optimized the PyA on the S_1 PES, while performing the scan along the R_{C-O} bond. The S_1 excited state of PyA (see Figure 4b) is of π→π* character (blue line in Fig S11) and its energy increases slightly during the first stages of elongation (up to R_{C-O} of about 1.7 Å), where it crosses with dissociative n→π* state (red line). The ascending character of the S_1 state at the first stages of elongation makes the dissociation process unlikely. Furthermore, the trend of the S_1 state towards lower energies for larger π-conjugated systems observed in the comparison between Figure 3c and d, anticipates that this activation barrier will become larger for extended π-conjugated systems. Therefore, we may conclude that the electronic delocalization in the π-conjugated PyA system, along with the ordering of the excited states are responsible for different photochemical behaviour of the anhydride group. Overall, the extension of π-conjugation influences the ordering of

the excited states and the presence of a dissociative n→π* excited state as a first one (S_1) for TPPA makes its C–O dissociation energetically feasible. On the contrary, the existence of low lying stable π→π*, placed energetically below n→π* states, hinders the analogous reaction for BPA.

Conclusion

In conclusion, we reported a new light-induced reaction on a semiconductor surface that paves the way for the on-surface synthesis of novel nanomaterials with readily available technological prospects. The experimental validation of the reaction steps is accompanied by the rationalization of the relationship between π-conjugation and photochemical reactivity. We showed the light-induced decarboxylation and decarbonylation of TPPA on a semiconductor surface and the lack of response in the BPA. The presence of a π-conjugated core in the latter case alters the energy distribution of the excited states and reduces the likeliness of bond dissociation upon light irradiation. Our findings demonstrate the link between molecular structure, π-conjugation, and photochemical reactivity, offering insights into the design principles for light-induced reactions on surfaces.

Supporting Information

The authors have cited additional references within the Supporting Information.[43,44,46–63]

Acknowledgements

This work was supported by the European Union and the Czech Ministry of Education, Youth and Sports (Project: MSCA Fellowship CZ FZU I–CZ.02.01.01/00/22_010/0002906) and the Czech Science Foundation project no. 21–17194L and 20–13692X, as well as the REFRESH—Research Excellence For Region Sustainability and High-tech Industries project number CZ.10.03.01/00/22_003/0000048 via the Operational Programme Just Transition. We acknowledge support from the CzechNanoLab Research Infrastructure supported by MEYS CR (LM2023051). Funding by the Swiss National Science Foundation (Grant# 202775) is gratefully acknowledged. We acknowledge the Paul Scherrer Institut, Villigen, Switzerland for provision of synchrotron radiation beamtime at beamline PEARL of the SLS. Lukas Rotach (Empa) and Patrick Ascher (PSI) are gratefully acknowledged for their technical support during the experiments. Open Access publishing facilitated by Fyzikalni ustav Akademie ved Ceske republiky, as part of the Wiley - CzechELib agreement.

Conflict of Interest

The authors declare no conflict of interest.

Data Availability Statement

The data that support the findings of this study are available from the corresponding author upon reasonable request.

Keywords: On-surface synthesis · semiconductor surfaces · photochemistry · STM · XPS

[1] L. Grill, M. Dyer, L. Lafferentz, M. Persson, M. V. Peters, S. Hecht, *Nat. Nanotechnol.* **2007**, *2*, 687–691.
[2] S. Clair, D. G. de Oteyza, *Chem. Rev.* **2019**, *119*, 4717–4776.
[3] Q. Shen, H.-Y. Gao, H. Fuchs, *Nano Today* **2017**, *13*, 77–96.
[4] J. I. Mendieta-Moreno, B. Mallada, B. de la Torre, T. Cadart, M. Kotora, P. Jelínek, *Angew. Chem. Int. Ed.* **2022**, *61*, e202208010.
[5] J. Björk, C. Sánchez-Sánchez, Q. Chen, C. A. Pignedoli, J. Rosen, P. Ruffieux, X. Feng, A. Narita, K. Müllen, R. Fasel, *Angew. Chem. Int. Ed.* **2022**, *61*, e202212354.
[6] E. Pérez-Elvira, A. Barragán, Q. Chen, D. Soler-Polo, A. Sánchez-Grande, D. J. Vicent, K. Lauwaet, J. Santos, P. Mutombo, J. I. Mendieta-Moreno, B. de la Torre, J. M. Gallego, R. Miranda, N. Martín, P. Jelínek, J. I. Urgel, D. Écija, *Nat. Synth* **2023**, 1–12.
[7] P. B. Bennett, Z. Pedramrazi, A. Madani, Y.-C. Chen, D. G. de Oteyza, C. Chen, F. R. Fischer, M. F. Crommie, J. Bokor, *Appl. Phys. Lett.* **2013**, *103*, 253114.
[8] J. P. Llinas, A. Fairbrother, G. Borin Barin, W. Shi, K. Lee, S. Wu, B. Yong Choi, R. Braganza, J. Lear, N. Kau, W. Choi, C. Chen, Z. Pedramrazi, T. Dumslaff, A. Narita, X. Feng, K. Müllen, F. Fischer, A. Zettl, P. Ruffieux, E. Yablonovitch, M. Crommie, R. Fasel, J. Bokor, *Nat. Commun.* **2017**, *8*, 633.
[9] Z. Chen, A. Narita, K. Müllen, *Adv. Mater.* **2020**, *32*, 2001893.
[10] M. Kolmer, A. A. Ahmad Zebari, J. S. Prauzner-Bechcicki, W. Piskorz, F. Zasada, S. Godlewski, B. Such, Z. Sojka, M. Szymonski, *Angew. Chem. Int. Ed.* **2013**, *52*, 10300–10303.
[11] M. Kittelmann, P. Rahe, M. Nimmrich, C. M. Hauke, A. Gourdon, A. Kühnle, *ACS Nano* **2011**, *5*, 8420–8425.
[12] K. Sun, Y. Fang, L. Chi, *ACS Materials Lett.* **2021**, *3*, 56–63.
[13] M. Lackinger, *Dalton Trans.* **2021**, *50*, 10020–10027.
[14] H. D. Roth, *Angew. Chem. Int. Ed. Engl.* **1989**, *28*, 1193–1207.
[15] F. Palmino, C. Loppacher, F. Chérioux, *ChemPhysChem* **2019**, *20*, 2271–2280.
[16] A. Miura, S. De Feyter, M. M. S. Abdel-Mottaleb, A. Gesquière, P. C. M. Grim, G. Moessner, M. Sieffert, M. Klapper, K. Müllen, F. C. De Schryver, *Langmuir* **2003**, *19*, 6474–6482.
[17] A. Richter, V. Haapasilta, C. Venturini, R. Bechstein, A. Gourdon, A. S. Foster, A. Kühnle, *Phys. Chem. Chem. Phys.* **2017**, *19*, 15172–15176.
[18] D. Sloan, Y.-M. Sun, H. Ihm, J. M. White, *J. Phys. Chem. B* **1998**, *102*, 6825–6830.
[19] A. Basagni, L. Ferrighi, M. Cattelan, L. Nicolas, K. Handrup, L. Vaghi, A. Papagni, F. Sedona, C. D. Valentin, S. Agnoli, M. Sambi, *Chem. Commun.* **2015**, *51*, 12593–12596.
[20] Q. Shen, J. H. He, J. L. Zhang, K. Wu, G. Q. Xu, A. T. S. Wee, W. Chen, *J. Chem. Phys.* **2015**, *142*, 101902.
[21] C. Nacci, M. Schied, D. Civita, E. Magnano, S. Nappini, I. Píš, L. Grill, *J. Phys. Chem. C* **2021**, *125*, 22554–22561.
[22] H.-Y. Gao, D. Zhong, H. Mönig, H. Wagner, P.-A. Held, A. Timmer, A. Studer, H. Fuchs, *J. Phys. Chem. C* **2014**, *118*, 6272–6277.
[23] L. Colazzo, F. Sedona, A. Moretto, M. Casarin, M. Sambi, *J. Am. Chem. Soc.* **2016**, *138*, 10151–10156.
[24] L. Grossmann, B. T. King, S. Reichlmaier, N. Hartmann, J. Rosen, W. M. Heckl, J. Björk, M. Lackinger, *Nat. Chem.* **2021**, *13*, 730–736.

[25] R. Lindner, P. Rahe, M. Kittelmann, A. Gourdon, R. Bechstein, A. Kühnle, *Angew. Chem. Int. Ed.* **2014**, *53*, 7952–7955.
[26] C.-A. Palma, K. Diller, R. Berger, A. Welle, J. Björk, J. L. Cabellos, D. J. Mowbray, A. C. Papageorgiou, N. P. Ivleva, S. Matich, E. Margapoti, R. Niessner, B. Menges, J. Reichert, X. Feng, H. J. Räder, F. Klappenberger, A. Rubio, K. Müllen, J. V. Barth, *J. Am. Chem. Soc.* **2014**, *136*, 4651–4658.
[27] F. Para, F. Bocquet, L. Nony, C. Loppacher, M. Féron, F. Cherioux, D. Z. Gao, F. Federici Canova, M. B. Watkins, *Nat. Chem.* **2018**, *10*, 1112–1117.
[28] X. Zhang, F. Gärisch, Z. Chen, Y. Hu, Z. Wang, Y. Wang, L. Xie, J. Chen, J. Li, J. V. Barth, A. Narita, E. List-Kratochvil, K. Müllen, C.-A. Palma, *Nat. Commun.* **2022**, *13*, 442.
[29] E. K. Fields, S. Meyerson, *Chem. Commun.* **1965**, 474–476.
[30] G. Porter, J. I. Steinfeld, *J. Chem. Soc. A* **1968**, 877.
[31] J. Lohmann, *J. Chem. Soc. Faraday Trans. 1* **1972**, *68*, 814.
[32] H. A. Weimer, B. J. McFarland, S. Li, W. Weltner, *J. Phys. Chem.* **1995**, *99*, 1824–1825.
[33] T. Sato, M. Moriyama, H. Niino, A. Yabe, *Chem. Commun.* **1999**, 1089–1090.
[34] T. Yatsuhashi, N. Nakashima, *J. Phys. Chem. A* **2000**, *104*, 203–208.
[35] D. Pérez, D. Peña, E. Guitián, *Eur. J. Org. Chem.* **2013**, *2013*, 5981–6013.
[36] F. Frezza, A. Sánchez-Grande, M. Ondráček, M. Vondráček, Q. Chen, O. Stetsovych, V. Villalobos-Vilda, E. Tosi, F. J. Palomares, M. F. López, C. Sánchez-Sánchez, K.-H. Ernst, J. A. Martín-Gago, J. Honolka, P. Jelínek, *J. Phys. Condens. Matter* **2023**, *35*, 335001.
[37] A. L. Rheingold, R. L. Durney, *J. Crystallogr. Spectrosc. Res.* **1987**, *17*, 127–134.
[38] M. V. Sulleiro, S. Quiroga, D. Peña, D. Pérez, E. Guitián, A. Criado, M. Prato, *Chem. Commun.* **2018**, *54*, 2086–2089.
[39] Y. Zou, L. Kilian, A. Schöll, T. Schmidt, R. Fink, E. Umbach, *Surf. Sci.* **2006**, *600*, 1240–1251.
[40] N. Pavliček, B. Schuler, S. Collazos, N. Moll, D. Pérez, E. Guitián, G. Meyer, D. Peña, L. Gross, *Nature Chem* **2015**, *7*, 623–628.
[41] J. K. Fremerey, *Vacuum* **1999**, *53*, 197–201.
[42] P. A. Redhead, *AIP Conf. Proc.* **2003**, *671*, 243–254.
[43] T. H. Dunning Jr, *J. Chem. Phys.* **1989**, *90*, 1007–1023.
[44] R. A. Kendall, T. H. Dunning Jr, R. J. Harrison, *J. Chem. Phys.* **1992**, *96*, 6796–6806.
[45] S. E. Braslavsky, *Pure Appl. Chem.* **2007**, *79*, 293–465.
[46] F. J. Giessibl, *Rev. Sci. Instrum.* **2019**, *90*, 011101.
[47] I. Horcas, R. Fernández, J. M. Gómez-Rodríguez, J. Colchero, J. Gómez-Herrero, A. M. Baro, *Rev. Sci. Instrum.* **2007**, *78*, 013705.
[48] M. Muntwiler, J. Zhang, R. Stania, F. Matsui, P. Oberta, U. Flechsig, L. Patthey, C. Quitmann, T. Glatzel, R. Widmer, E. Meyer, T. A. Jung, P. Aebi, R. Fasel, T. Greber, *J. Synchrotron Radiat.* **2017**, *24*, 354–366.
[49] V. Blum, R. Gehrke, F. Hanke, P. Havu, V. Havu, X. Ren, K. Reuter, M. Scheffler, *Comput. Phys. Commun.* **2009**, *180*, 2175–2196.
[50] J. P. Perdew, K. Burke, M. Ernzerhof, *Phys. Rev. Lett.* **1996**, *77*, 3865–3868.
[51] A. Tkatchenko, M. Scheffler, *Phys. Rev. Lett.* **2009**, *102*, 073005.
[52] A. D. Becke, *J. Chem. Phys.* **1993**, *98*, 5648–5652.
[53] P. J. Stephens, F. J. Devlin, C. F. Chabalowski, M. J. Frisch, *J. Phys. Chem.* **1994**, *98*, 11623–11627.
[54] O. Krejčí, P. Hapala, M. Ondráček, P. Jelínek, *Phys. Rev. B* **2017**, *95*, 045407.
[55] P. Hapala, G. Kichin, C. Wagner, F. S. Tautz, R. Temirov, P. Jelínek, *Phys. Rev. B* **2014**, *90*, 085421.
[56] P. Hapala, R. Temirov, F. S. Tautz, P. Jelínek, *Phys. Rev. Lett.* **2014**, *113*, 226101.
[57] A. Schäfer, H. Horn, R. Ahlrichs, *J. Chem. Phys.* **1992**, *97*, 2571–2577.
[58] A. Schäfer, C. Huber, R. Ahlrichs, *J. Chem. Phys.* **1994**, *100*, 5829–5835.
[59] M. J. Frisch, G. W. Trucks, H. B. Schlegel, G. E. Scuseria, M. A. Robb, J. R. Cheeseman, G. Scalmani, V. Barone, G. A. Petersson, H. Nakatsuji, X. Li, M. Caricato, A. V. Marenich, J. Bloino, B. G. Janesko, R. Gomperts, B. Mennucci, H. P. Hratchian, J. V. Ortiz, A. F. Izmaylov, J. L. Sonnenberg, D. Williams-Young, F. Ding, F. Lipparini, F. Egidi, J. Goings, B. Peng, A. Petrone, T. Henderson, D. Ranasinghe, V. G. Zakrzewski, J. Gao, N. Rega, G. Zheng, W. Liang, M. Hada, M. Ehara, K. Toyota, R. Fukuda, J. Hasegawa, M. Ishida, T. Nakajima, Y. Honda, O. Kitao, H. Nakai, T. Vreven, K. Throssell, J. A. Montgomery, Jr., J. E. Peralta, F. Ogliaro, M. J. Bearpark, J. J. Heyd, E. N. Brothers, K. N. Kudin, V. N. Staroverov, T. A. Keith, R. Kobayashi, J. Normand, K. Raghavachari, A. P. Rendell, J. C. Burant, S. S. Iyengar, J. Tomasi, M. Cossi, J. M. Millam, M. Klene, C. Adamo, R. Cammi, J. W. Ochterski, R. L. Martin, K. Morokuma, O. Farkas, J. B. Foresman, and D. J. Fox, Gaussian 16, Revision C.01, Gaussian, Inc., Wallingford CT, **2016**.
[60] J. Schirmer, *Phys. Rev. A* **1982**, *26*, 2395–2416.
[61] A. B. Trofimov, J. Schirmer, *J. Phys. B* **1995**, *28*, 2299.
[62] S. G. Balasubramani, G. P. Chen, S. Coriani, M. Diedenhofen, M. S. Frank, Y. J. Franzke, F. Furche, R. Grotjahn, M. E. Harding, C. Hättig, A. Hellweg, B. Helmich-Paris, C. Holzer, U. Huniar, M. Kaupp, A. Marefat Khah, S. Karbalaei Khani, T. Müller, F. Mack, B. D. Nguyen, S. M. Parker, E. Perlt, D. Rappoport, K. Reiter, S. Roy, M. Rückert, G. Schmitz, M. Sierka, E. Tapavicza, D. P. Tew, C. van Wüllen, V. K. Voora, F. Weigend, A. Wodyński, J. M. Yu, *J. Chem. Phys.* **2020**, *152*, 184107.
[63] TURBOMOLE V7.5 2020, a development of University of Karlsruhe and Forschungszentrum Karlsruhe GmbH, 1989–2007, TURBOMOLE GmbH, since **2007**, https://www.turbomole.org.

Manuscript received: March 28, 2024
Accepted manuscript online: May 3, 2024
Version of record online: ■■, ■■

Research Articles

On-Surface Synthesis

F. Frezza, A. Sánchez-Grande,* S. Canola, A. Lamancová, P. Mutombo, Q. Chen, C. Wäckerlin, K.-H. Ernst, M. Muntwiler, N. Zema, M. Di Giovannantonio,* D. Nachtigallová,* P. Jelínek*

Controlling On-Surface Photoactivity: The Impact of π-Conjugation in Anhydride-Functionalized Molecules on a Semiconductor Surface

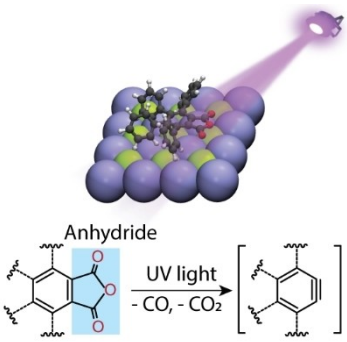

This work presents the on-surface reaction of anhydride-functionalized molecules as precursors on a SnSe surface investigated by SPM and XPS techniques. Quantum chemical calculations demonstrate how their photoactivity can be controlled by modulating the π-conjugation of the molecular core.